FOUNDATIONS OF CIVIL AND ENVIRONMENTAL ENGINEERING

No. 7 2006

Russell A. GREEN, Radoslaw L. MICHALOWSKI*
University of Michigan, Ann Arbor, USA

SHEAR BAND FORMATION BEHIND RETAINING STRUCTURES SUBJECTED TO SEISMIC EXCITATION

Received: 21 June 2006
Accepted: 3 August 2006

The behaviour of soil retaining structures during earthquakes is investigated. Seismic excitation imparts inertial forces to the soil retaining system, and, once the seismic acceleration reaches the yield level, the structure exhibits permanent displacements. This is typically associated with appearance of a shear band in the backfill. The application of the kinematic approach of limit analysis is briefly discussed. A specific example of a retaining wall with one distinct shear band is then presented. The inclination of the shear band is found to be dependent on the acceleration amplitude of the seismic excitation, per classical earth pressure theory. Also, it was found that the inclination of the shear band does not remain stationary, but rather changes throughout the shaking in response to the variation in the acceleration amplitude of the excitation. This phenomenon is illustrated by results from both a physical experiment and a numerical prediction, which indicate a distinct change in the shear band inclination during seismic excitation, leaving a clear pattern of "shear banding".

Key words: seismic excitation, earthquake, yield acceleration, shear band, retaining wall displacement, plasticity analysis

1. INTRODUCTION

Seismic excitation of earth structures has been considered for eight decades now. Most methods used to determine permanent displacements involve

* Corresponding author. Tel.: 001 734 763-2146; fax: 001 734 764-4292.
E-mail address: rlmich@umich.edu (R. L. Michalowski)

ISSN 1642-9303

simplified techniques where the soil is modelled as a block sliding on a failure surface (or a shear band) formed in the soil [2,13]. Though relatively simple, this model is quite effective and was implemented in engineering practice more than four decades ago [10,14]. Early experiments included the sliding of a soil mass along a pre-determined surface [13]. However, unlike static failures, the geometry of the collapse mechanism of a seismically excited structure is not an exclusive function of material properties and the topology of the structure. Rather, the geometry is also a function of the earthquake excitation, and the geometry may change during earthquake shaking in response to the variation in ground acceleration.

Herein, an analysis method is proposed for calculating the displacements of earth structures subjected to seismic excitation. This method has many common components with the traditional single block technique; however, it takes into account the non-associativity of the flow of granular soils and can be generalized for any number of blocks. Furthermore, the proposed method becomes tractable through the introduction of the acceleration hodograph.

Regarding the organization of the remainder of this paper, first, the proposed method is briefly discussed in general form, followed by the adaptation of the technique to retaining walls subjected to earthquake motions. Next, the proposed method is discussed in context of the analytical solution to shear band inclination, and observations from physical and numerical model results are presented.

2. DISPLACEMENTS OF SEISMICALLY LOADED STRUCTURES

When the ground acceleration reaches the yield acceleration of a structure the process of plastic deformation is initiated. The yield acceleration can be determined using limit analysis as described in a recent paper by Michalowski [8]. The approach is based on the kinematic theorem of limit analysis (i.e., in any kinematically admissible failure mechanism, the rate of internal work is not less than the rate of true external forces). This theorem holds for materials with convex yield surfaces and with deformation governed by the normality rule. Introducing a kinematically admissible velocity field v_i and associated stress field σ_{ij}, both marked with superscript k, this theorem can be written as:

$$\int_V \sigma_{ij}^k \dot{\varepsilon}_{ij}^k dV \geq \int_S T_i v_i dS + \int_V X_i v_i^k dV \tag{2.1}$$

where, T_i is the traction on boundary S, and X_i are the distributed forces in mechanism volume V. In seismic problems, the last term includes both the

gravity forces and the inertial forces caused by earthquake excitation. Stress field σ_{ij}^{k} is compatible with the selected collapse mechanism, but is not necessarily in equilibrium.

The slope shown in Fig. 1 is now introduced and is brought to plastic state by horizontal earthquake acceleration. The upper bound to the yield acceleration can be found from inequality (2.1), where the only work dissipation occurs along the velocity discontinuities (left-hand side); traction T_i is zero on the slope boundary; and the distributed load is the gravity force and the inertial horizontal force ($k_h mg$). In this latter term, k_h is the horizontal inertial coefficient, m is the mass of a given block in the postulated mechanism, and g is the acceleration due to gravity. The most adverse case (in the absence of vertical shaking) is when the ground acceleration is directed *into* the slope (i.e., to the right in Fig. 1a), and hence, the seismically induced inertial forces are directed *away from* the slope. Consequently, for a given collapse mechanism, k_h is the only unknown variable in theorem (2.1). As this approach gives the upper bound yield acceleration, the minimum k_h is sought, with the geometry of the mechanism being variable.

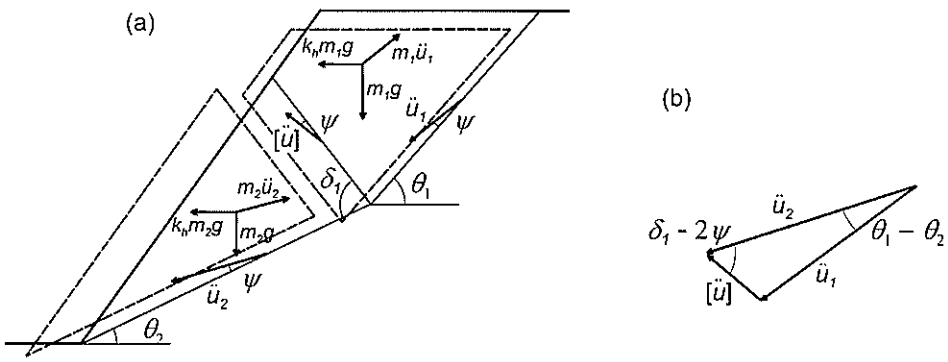

Fig. 1. Collapse of a slope (after [8]): (a) acceleration field, and (b) acceleration hodograph.

It needs to be emphasized that the accelerations in Fig. 1 are not time derivatives of the velocity field v_i in the admissible failure mechanism used in theorem (2.1). The reader is referred to the recent paper by Michalowski [8] for a detailed discussion of the intricacies of this approach.

In a kinematically admissible mechanism, the velocity "jump" vectors are inclined at angle of internal friction ϕ to the velocity discontinuities. Expanding the mechanism to n blocks, the velocities of the blocks, v_1, v_2, v_3, ... , v_n, can be described as:

$$v_i = v_1 \prod_{k=2}^{k=i} \frac{\sin(\delta_k - 2\phi + \theta_{k-1} - \theta_k)}{\sin(\delta_k - 2\phi)}, \qquad \begin{matrix} k = 2,3,4...i \\ i = 2,3,4...n \end{matrix} \tag{2.2}$$

with angles θ and δ defined in Fig. 1, and v_1 being the velocity of block 1 (kinematic boundary condition). The velocities in eq. (2.2) are incipient velocities, and they conform to the normality rule. The accelerations in Fig. 1, however, generally conform to a non-associative flow rule governed by dilation angle ψ, and they can be found directly from the geometrical relations on the hodograph, Fig. 1(b):

$$\ddot{u}_i = \ddot{u}_1 \prod_{k=2}^{k=i} \frac{\sin(\delta_k - 2\psi + \theta_{k-1} - \theta_k)}{\sin(\delta_k - 2\psi)}, \qquad \begin{matrix} k = 2,3,4...i \\ i = 2,3,4...n \end{matrix} \tag{2.3}$$

where, ψ is the dilatancy angle. The "true" velocities and displacements of the blocks in the mechanisms are the first and second integrals over time, respectively, of accelerations $\ddot{u}_i$.

When the seismic acceleration reaches its yield level k_y, the balance of work rate during incipient failure (in the absence of vertical shaking) is:

$$D = \dot{W}_\gamma + k_y g \sum_{i=1}^{n} m_i v_i \cos(\theta_i - \phi) \tag{2.4}$$

where, m_i is the mass of *i-th* block; $\dot{W}_\gamma$ is the rate of work of gravity forces; and D is the rate of work dissipation in the entire mechanism. Once the horizontal acceleration exceeds the yield level, the structure deforms plastically, but the work rate balance equation now has an additional term due to inertial forces. As the inertial force due to acceleration in a given block is opposite in direction to $\ddot{u}_i$, the work rate of this force is negative, however it is written below on the left-hand side with a positive sign:

$$D + \cos(\phi - \psi) \sum_{i=1}^{n} m_i \ddot{u}_i v_i = \dot{W}_\gamma + kg \sum_{i=1}^{n} m_i v_i \cos(\theta_i - \phi) \tag{2.5}$$

Subtracting eq. (2.4) from (2.5), and after several transformation, one obtains the acceleration of the *n-th* block as:

$$\ddot{u}_n = g(k - k_y)C \tag{2.6}$$

where C is a function of the geometry of the failure mechanism, the soil properties, and the yield acceleration [9]. The displacement of the *n-th* block (u_n)

is the second integral of eq. (2.6) over time intervals when the first integral (velocity) is positive:

$$u_n = C \int_t \int_t g(k - k_y)\, dtdt, \qquad v_n > 0 \tag{2.7}$$

From a practical view point, this equality is very convenient since coefficient C is independent of the earthquake motion. Hence, the integral of $g(k - k_y)$ can be calculated for a given acceleration time history and for a variety of yield accelerations, and can be used as a design tool.

While the procedure described in this section can be easily implemented, it is not directly applicable to the seismic analysis of earth retaining structures. This is because both physical and numerical test results of such structures show that the mechanism evolves throughout the seismic excitation. More specifically, the observed mechanism is simple in that the structure appears to have only two distinct regions of rigid motion, but the shear band defining the moving soil evolves in response to the variation in the amplitude of the acceleration during the seismic shaking. The next two sections focus on this issue.

3. COLLAPSE MECHANISM OF A RETAINING STRUCTURE SUBJECTED TO SEISMIC LOAD

Physical model tests by Aitken [1] of a retaining wall system showed a two block failure mechanism, similar to the schematic in Fig. 2. The method proposed in the previous section can be easily adapted to such a mechanism by introducing the wall-soil interface friction angle ϕ_w, Fig. 2.

This is an incipient mechanism used to calculate the yield acceleration, but the true deformation may be governed by the non-associative law with an appropriate dilatancy angle ψ of the soil, and possibly incompressible sliding at the wall interface. The accelerations of the soil and wall system are shown in Fig. 3, and they are collinear with true velocities, not the incipient ones in Fig. 2.

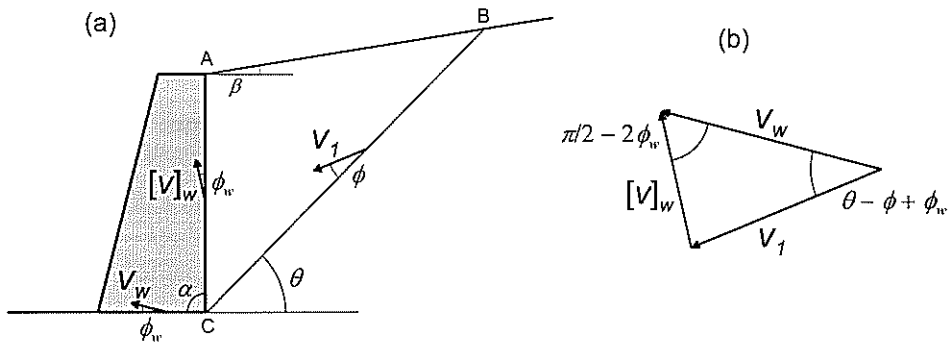

Fig. 2. Failure of a vertical ($\alpha = \pi/2$) retaining wall: (a) mechanism, and (b) hodograph.

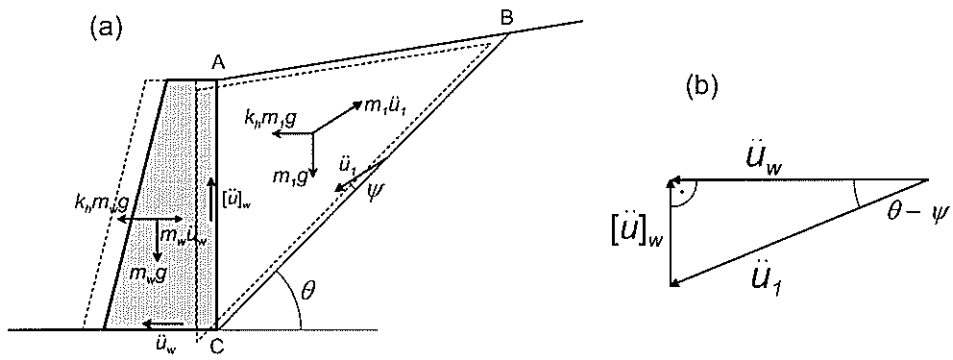

Fig. 3. (a) Accelerations of the soil and retaining wall, (b) acceleration hodograph.

This mechanism appears to be a reasonable adaptation of the more general mechanism discussed in Section 2. However, the physical model tests [1] revealed that the failure surface (or the shear band) *BC* in Fig. 2(a) is not stationary throughout the duration of seismic shaking. This will be discussed in Sections 4.2 and 4.3, and a proposal to accommodate the non-stationary location of the shear band will be discussed in Section 5.

4. SHEAR BAND INCLINATION BEHIND A RETAINING WALL

In calculating the load imposed on a retaining wall, the angle θ in the mechanism in Fig. 2(a) needs to be chosen such that the calculated yield acceleration is minimal. This is because the kinematic approach of limit analysis yields an upper bound to an active force, and the seismically induced inertial

force ($k_h m_1 g$) in Fig. 3 is an active force. However, when the earthquake acceleration exceeds the yield acceleration, the work rate in the system will no longer be balanced if deformation occurs according to the same mechanism, and, in the absence of additional external forces, the mechanism likely evolves to ensure the work balance. We discuss this issue in Section 4.2 in view of experimental results and another possible interpretation of these results. However, first, an expression for angle θ is derived for an arbitrary horizontal acceleration in Section 4.1.

4.1. Analytical solution to shear band inclination

An early solution to the load on a wall with arbitrary inclination was developed by Poncelet [12]. He devised an ingenious graphical method for finding an optimum solution to the load exerted on the wall. This graphical method was used by the authors to determine the inclination angle θ (Fig. 2(a)) of the failure surface as a function of horizontal acceleration:

$$\tan\theta = \frac{\sin(\beta+\theta')\sqrt{\dfrac{\sin(\phi+\phi_w)\sin(\alpha-\phi_w-\theta')}{\sin(\phi-\beta-\theta')\sin(\alpha+\beta)}}+\sin(\alpha-\phi-\phi_w-\theta')}{\cos(\beta+\theta')\sqrt{\dfrac{\sin(\phi+\phi_w)\sin(\alpha-\phi_w-\theta')}{\sin(\phi-\beta-\theta')\sin(\alpha+\beta)}}-\cos(\alpha-\phi-\phi_w-\theta')} - \theta' \quad (4.1)$$

where, θ' is dependent on the horizontal and vertical acceleration coefficients k_h and k_v:

$$\theta' = \arctan\frac{k_h}{1-k_v} \quad (4.2)$$

and the other angles are indicated in Fig. 2(a). In a different form, the very same angle was obtained analytically by Okabe [11] in the 1920's.

In typical design calculations for retaining structures, one seeks the load imposed on the wall by the soil. The wall itself then is not part of the analysis. In calculations focused on the displacements caused by seismic loads, the wall needs to be part of the system, and angle θ calculated from eq. (4.1) may not necessarily depict the inclination of the true shear band appearing in the backfill. One might make an intuitive conjecture, however, that this inclination does not depart far from eq. (4.1). The specific issue this paper is focused on is: does the shear band behind the wall remain stationary throughout the earthquake shaking?

4.2. Earlier experimental work

A series of small scale shake table tests were performed on a retaining wall system by Aitken [1]. A post-test photo is shown in Fig. 4; for scale, the height of the retaining wall shown in this photo is 0.32 m. The foundation and backfill soil was New Brighton sand, which is a uniform, medium-to-fine grained sand. The model was constructed by first placing the foundation sand into the test box. The foundation sand was densified using high frequency vibrations, and then screed level. The wall was placed on the foundation sand and the backfill put in place. The backfill was densified using high frequency vibrations and then screed level.

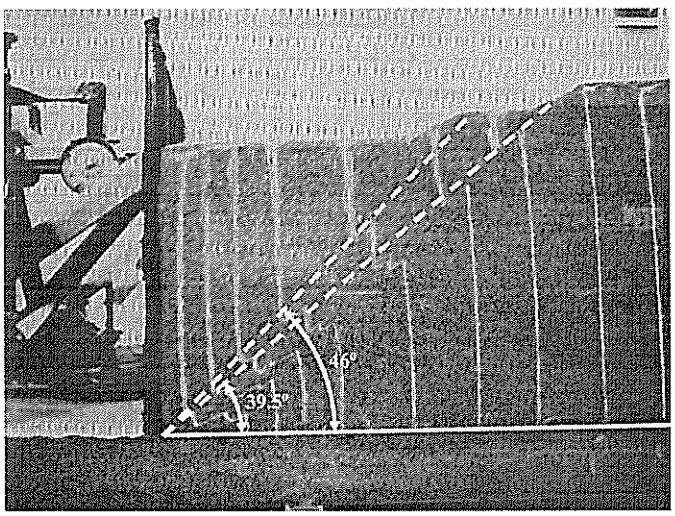

Fig. 4. A post-test photograph of the small scale shake table model of a retaining wall system (after [1]).

The model was subjected to horizontal base excitations that were generated by a lever arm-spring release mechanism. The excitations were decaying sine waves whose first two to three cycles exceeded the yield acceleration (Fig.
Fig.5(a)). As a result of the shaking, two predominant shear bands formed behind the wall, as denoted by the white dashed lines in Fig. 4. One of the shear bands is inclined 39.5° from the horizontal, and the other 46°. Other shear bands at other angles of inclination may also be observed in Fig. 4, as indicated by the offsets in the vertical white sand lines in the backfill. However, these other shear bands did not fully develop (i.e., they do not extend all the way from the heel of the wall to the free surface).

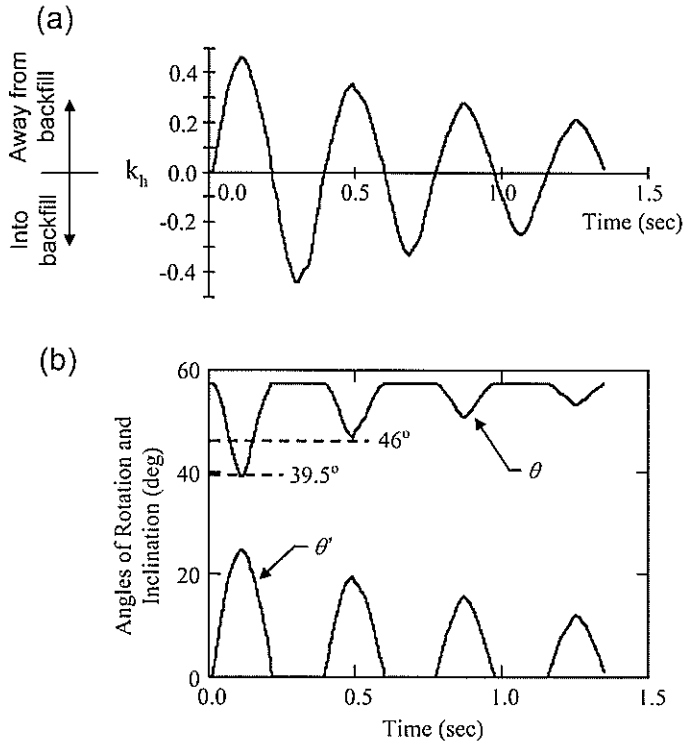

Fig.5.(a)Time history of the horizontal inertial coefficient induced by the base excitations, (b) Time histories of θ' and θ computed using eqs. (4.1) and (4.2) for the inertial load away from the backfill.

Using eqs. (4.1) and (4.2) in conjunction with the excitation time history shown in Fig.
Fig.5(a), the angles of rotation (θ') that would induce the same inertial force as the horizontal base excitation and the corresponding angles of inclination (θ) of the potential shear bands were computed and plotted in Fig.
Fig.5(b). In computing θ, the following parameter values were used: $\alpha = 90°$, $\beta = 0°$, and $k_v = 0$. Additionally, because sand paper having a similar grit to the New Brighton sand was adhered to the base and stem of the wall, it was assumed that $\phi_w = \phi$. Aitken [1] performed a series of simple shear tests to determine ϕ as a function of density and confining stress; from the range of results from these tests, $\phi = 35°$ was assumed by the authors in computing θ.

As may be observed from Fig.
Fig.5(b), the angle of inclination (θ) of the potential shear band decreases as the induced inertial force increases and that the upper value for θ (~58°) corresponds to that predicted by the Coulomb method for active (static) conditions.

Superimposed on the plot of the time history for θ are the angles of inclination of the two predominant shear bands identified in the photo of the post-test results of the model retaining wall (Fig. 4). As may be observed, these angles are in close accord with those predicted by eq. (4.1). Aitken [1] did not give the mass of the retaining wall used in his study, and consequently, the yield acceleration cannot be computed. However, from his test results, $k_y \approx 0.3$, thus precluding the formation of shear bands from the third and fourth cycles in the base excitation.

4.3. Numerical results

A series of non-linear dynamic response analyses were performed on the cantilever wall using the finite difference program *FLAC* [7]. The geometry and structural detailing of the wall analyzed were determined following the US Army Corps of Engineers static design procedures. The retaining wall was 6.1 m in height, retaining medium-dense, cohesionless, compacted fill. Both the foundation and backfill soils were modelled as being elasto-plastic with Mohr-Coulomb failure criterion, and interface elements were used between the wall and the soil to allow relative movements and permanent displacements in the wall-soil system to occur. The wall and backfill were numerically constructed in 0.6 m lifts, allowing for equilibrium of the stresses to occur between lift placements. Additional details of the wall design and *FLAC* modelling are presented in [3,4,5,6].

The deformed mesh from one of the numerical analyses is shown in Fig. 6. As may be observed from this figure, a series of shear bands at varying angles of inclination formed in the backfill (Note: White lines were superimposed on the deformed mesh to highlight the shear bands.).

Fig. 6. Deformed mesh of a cantilever retaining wall system subjected to seismic

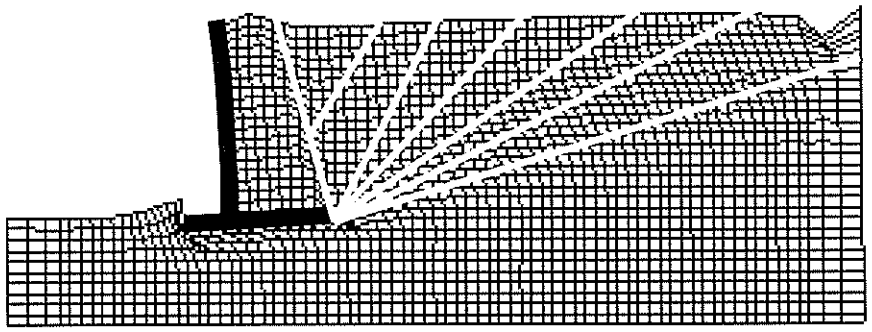

excitations (after [5]).

The response of the retaining wall system shown in Fig. 6 was more complex than the physical model test discussed previously because the

stem of the wall was allowed to bend and the entire wall was allowed to rotate in response to the induced inertial forces. However, the multiple shear bands in the backfill are consistent with the physical model test results shown in Fig. 4 and with eqs. (4.1) and (4.2).

5. SEISMIC DISPLACEMENT OF RETAINING WALLS

The proposed method for calculating the displacements of retaining walls subjected to seismic excitation outlined in Section 2 leads to a convenient formula in eq. (2.7). While this method is applicable to both slopes and walls, experiments on walls (both physical and numerical) indicate that the shear band that forms in the backfill is not stationary. Rather, one shear band can be associated with one cycle of seismic excitation, and if the subsequent cycle has a distinctly different peak acceleration, a new shear band can form at a different inclination angle. This observation suggests that under a "synthetic" sinusoidal excitation having uniform amplitude, only one shear band will appear, whereas for an actual earthquake excitation multiple shear bands will likely form. Further studies are needed to reveal the impact of the frequency of the excitation on the formation of multiple shear bands, and the possible influence of strain softening of the backfill.

6. FINAL REMARKS

The classical sliding-block concept [10,14] can be adapted to include more complex failure mechanisms experienced by earth structures. In applying this concept to retaining walls, two observations were made: the backfill can be modeled with good accuracy with only one block, but the geometry of the block changes during the process of shaking in response to the variation in the amplitude of the excitation. This is because the inclination of the shear band is dependent on the induced inertial force, and hence, on the seismic acceleration. This last statement is supported by considerations based on the classical quasi-static theory. It is then reasonable to expect that a new shear band forms at the peak of the acceleration in a cycle (or slightly after), and becomes visible only once the displacements are large enough to be noticeable. One would also expect that if the excitation has uniform amplitude, sliding will occur along one shear band. Future research will include testing, both physical and numerical, to gain more insight into formation of shear bands in the soil during ground motion, the influence of ground motion frequency, and the role of strain softening of the soil.

ACKNOWLEDGMENTS

A portion of the work presented in this paper was carried out while Prof. Michalowski was supported by the Army Research Office, grant No. DAAD19-03-1-0063. The remaining work was carried out while Prof. Green was supported by the Headquarters, US Army Corps of Engineers (HQUSACE) Civil Works Earthquake Engineering Research Program (EQEN). Dr. Robert M. Ebeling was the cognizant Corps representative. This support is greatly appreciated. The authors also acknowledge ITASCA Consulting Group, Inc., for the academic loan of their *FLAC* code. This collaboration is very much appreciated.

REFERENCES

1. Aitken, G.H.: Seismic response of retaining walls. MS Thesis, University of Canterbury, Christchurch, New Zealand 1982.
2. Goodman, R.E., Seed, H.B.: Earthquake-induced displacements in sand embankments, J. Soil Mech. Found. Div., 92 (2) (1966) 125-146.
3. Green, R.A., Ebeling, R.M.: Seismic Analysis of Cantilever Retaining Walls, Phase 1, Technical Report ERDC/ITL TR-02-3, US Army Corps of Engineers Engineering Research and Development Center, Vicksburg, MS, (2002) 104pp.
4. Green, R.A., Ebeling, R.M.: Modeling the Dynamic Response of Cantilever Earth-Retaining Walls Using *FLAC*, Proc., 3rd International Symposium on *FLAC* and *FLAC*^{3D} Numerical Modeling in Geomechanics (R. Brummer, P. Andrieux, C. Detournay, and R. Hart, eds.), A.A. Balkema Publishers: (2003) 333-342.
5. Green, R.A., Olgun, C.G., Ebeling, R.M., Cameron, W.I.: Seismically Induced Lateral Earth Pressures on a Cantilever Retaining Wall, Advancing Mitigation Technologies and Disaster Response for Lifeline Systems (J.E. Beavers, ed.), ASCE Technical Council on Lifeline Earthquake Engineering Monograph No. 25 (2003) 946-955.
6. Green, R.A., Olgun, C.G., Cameron, W.I.: The Dynamic Response of Cantilever Retaining Walls Subjected to Earthquake Motions, Proc. 23rd Southeastern Conference on Theoretical and Applied Mechanics (M.A. Pando, F.J. Acosta, and L.E. Suarez, eds.), Mayagüez, Puerto Rico, May 21 – 23, (2006) 14 pp.
7. Itasca Consulting Group: *FLAC, Fast Lagrangian Analysis of Continua, User's Manual.* Minneapolis, Minnesota, USA, 1997.

8. Michalowski, R.L.: Displacements of multi-block geotechnical structures subjected to seismic excitation, J. Geotech. Geoenv. Eng., (2006) in review.
9. Michalowski, R.L., You, L.: Displacement of reinforced slopes subjected to seismic loads, J. Geotech. Geoenv. Eng., 126 (8) (2000) 685-694.
10. Newmark, N.M.: Effects of earthquakes on dams and embankments. Géotechnique, London, 15 (1965) 139-160.
11. Okabe, S.: General theory on earth pressure and seismic stability of retaining wall and dam, J. Japan. Soc. Civil Eng., 10 (6) (1924) 1277-1323.
12. Poncelet, J.V. Mémoire sur la stabilité des revêtements et de leurs fondations. Mém. de l'officier du génie. 13 (1840) 7-226.
13. Seed, H.B., Goodman, R.E.: Earthquake stability of slopes of cohesionless soils, J. Soil Mech. Found. Div., 90 (6) (1964) 43-73.
14. Whitman, R.V.: Letters to the Army Engineer Division, South Pacific, dated: 14 April 1953, 19 May 1953, and 20 May 1953.